

<sup>11</sup>Wattendorf, F., "Study of the Effect of Curvature on Fully Developed Turbulent Flow," *Proceedings of The Royal Society*, Vol. A148, 1935, pp. 568-598.

<sup>12</sup>Spangenberg, W. G., Rowland, W. R., and Mease, N. E., "Measurements in a Turbulent Boundary Layer Maintained in a Nearly Separated Condition," *Fluid Mechanics of Internal Flow*, Elsevier, New York, 1967, pp. 110-151.

<sup>13</sup>Clauser, F. H., "Turbulent Boundary Layers in Adverse Pressure Gradients," *Journal of Aeronautical Sciences*, Vol. 21, Feb. 1954, pp. 91-108.

<sup>14</sup>Ludwig, H. and Tillmann, W., "Investigations of the Wall Shearing Stress in Turbulent Boundary Layers," TM 1285, 1950, NACA.

<sup>15</sup>Townsend, A. E., "The Behaviour of a Turbulent Boundary Layer near Separation," *Journal of Fluid Mechanics*, Vol. 12, April 1962, pp. 536-554.

<sup>16</sup>Thompson, B. G. J., "A New Two-Parameter Family of Mean Velocity Profiles for Incompressible Turbulent Boundary Layers on Smooth Walls," R&M 3463, 1967, Aeronautical Research Council, London, England.

## Dynamics of Slung Bodies Using a Single-Point Suspension System

Corrado Poli\* and Duane Cromack†  
University of Massachusetts, Amherst, Mass.

A stability analysis of slung bodies of current, practical interest, and the identification of the towing system parameters which affect stability is presented. The analysis is accomplished by first determining the aerodynamic characteristics of two nonstreamlined bodies; an 8 ft × 8 ft × 20 ft cargo container, and a 20-ft-long, 5.4-ft-diam right-circular cylinder. These results are then used in a linearized small-perturbation stability analysis of the slung system. For the single-point system, it is shown that long cables, high speeds, and light loads are required for stability. The drag-to-weight ratio of the towed body and the length of the cable are shown to be the most important stability parameters.

### Nomenclature

$a, h$	= horizontal and vertical distances between attachment points
$A, B, C$	= moments of inertia of the towed body about the $x, y, z$ axes
$D/W$	= drag-to-weight ratio
$d_1, d_2$	= distance from c.g. of slung load to the attachment point, measured in the XYZ system (primed quantities are measured in xyz system)
$l$	= cable length
$L, M, N$	= aerodynamic moments
$m$	= mass of the towed body
$r/w$	= edge radius-to-body width ratio
$T_0$	= steady-state cable force
$u, v, w$	= linear perturbation
$U_0$	= steady-state velocity
$X, Y, Z$	= aerodynamic forces
$\theta, \psi, \phi$	= aircraft Euler angles
$\alpha$	= angle of attack
$\beta$	= side-slip angle
$\gamma$	= steady-state tow angle (Fig. 3)
$C_D$	= drag coefficient
$C_L$	= lift coefficient
$C_Y$	= side-force coefficient
$C_l$	= roll moment coefficient (moment measured about c.g.)
$C_m$	= pitch moment coefficient (moment measured about c.g.)
$C_n$	= yaw moment coefficient (moment measured about c.g.)
$C_{L\alpha}$	= $\partial C_L / \partial \alpha$
$C_{m\alpha}$	= $\partial C_m / \partial \alpha$
$C_{y\beta}$	= $\partial C_Y / \partial \beta$

$C_n$	= $\partial C_n / \partial \beta$
$X_u, X_w$ , etc.	= changes in the aerodynamic forces and moments due to changes in velocity
$Re$	= Reynolds Number

### Introduction

IN 1930, Glauert<sup>1</sup> performed what appears to be the first comprehensive study into the dynamics of towed bodies when he investigated the lateral and longitudinal stability of a nonlifting body towed by a light inextensible wire. While additional valuable work has been done in the area of airborne towing<sup>2-15</sup> (Ref. 12 should be consulted for a comprehensive survey), a study of the available literature shows that few quantitative results are available for the dynamic state during the towing of nonaerodynamic shaped bodies, such as a palletized cargo, beneath rotary winged aircraft.

The increased importance of towing becomes clear when one begins to imagine conditions when it would become desirable to transport some heavy operational equipment from one remote and inaccessible area of operation to another, or even from sea to land. One way, and in some cases possibly the only way, to perform quickly this transportation of equipment would be to have a helicopter tow the gear from one region to another. It is also conceivable that towing of cargo could greatly reduce the costly delays in overseas shipping schedules often caused by inadequate or nonexistent port facilities in remote and underdeveloped areas where vessels could stand idle for weeks before their cargo can be unloaded. In such situations if the air-lifting of equipment is to be performed successfully, then the towing must be accomplished with a minimum amount of unstable motion. Hence, before a system can be considered operational, it is necessary to establish the ranges of operation in which instabilities are likely to occur.

The need for such investigations is quite clear. For instance, Etkin and Macworth<sup>5</sup> report of the serious instability which occurred when attempts were made to tow

Received June 15, 1972; presented as Paper 72-986 at the AIAA 2nd Atmospheric Flight Mechanics Conference, Palo Alto, Calif., September 11-13, 1972; revision received November 1, 1972. This work was supported by the U.S. Army Research Office—Durham.

Index category: VTOL Handling, Stability, and Control.

\*Professor, Mechanical and Aerospace Engineering Department. Member AIAA.

†Associate Professor, Mechanical and Aerospace Engineering Department. Member AIAA.

loads of dense material by helicopter to a remote construction site. Similarly, Shanks<sup>6-8</sup> showed experimentally that lateral instability problems can arise in towing parawing gliders and half-cone re-entry vehicles. Therefore, if towing is to be seriously considered as an effective operational mode of transportation further dynamic studies of these situations are necessary.

With the exception of the studies carried out by both Glauert<sup>1</sup> and Reid,<sup>10</sup> most investigators have restricted their analytical studies to either longitudinal motion<sup>4,11,13</sup>

or lateral motion.<sup>5,9</sup> Glauert and Reid's investigations, on the other hand, while quite general, contain few specific quantitative results. None of the previous studies have included a discussion of the aerodynamic characteristics of bluff bodies.

The objectives of this investigation, then, are the determination of the stability criteria of slung bodies of current, practical interest, and the identification of the towing systems parameters which affect stability. This will be accomplished by first determining the aerodynamic characteristics of two nonstreamlined bodies, an 8 ft × 8 ft × 20 ft cargo container, and a 20-ft-long, 5.4-ft-diam right-circular cylinder. These results will then be used in a linearized small-perturbation stability analysis of the slung system. Both the lateral and longitudinal degrees of freedom will be considered.

### Wind-Tunnel Tests

Wind-tunnel tests were conducted on two models, a rectangular box and a right-circular cylinder. Static force and moment coefficients were determined with typical results shown in Figs. 1 and 2. Tests confirmed the symmetry of flow for these models, hence the data presented in Figs. 1 and 2 may be interpreted as either side force vs side-slip angle or as lift vs angle of attack, etc. Additional tests were conducted on the box with fins of crucifix form and of three different sizes. Comparison of the box data

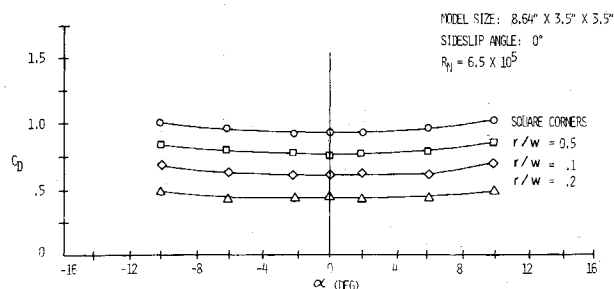


Fig. 1a Drag coefficient vs angle of attack for rectangular box—no fins.

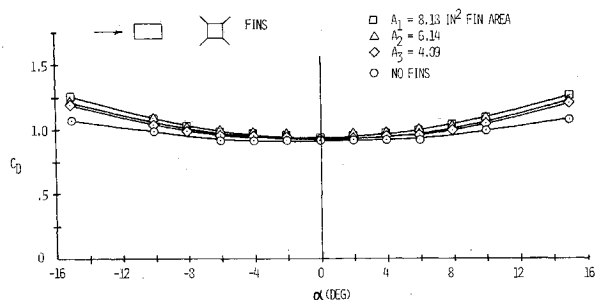


Fig. 1b Drag coefficient vs angle of attack for rectangular box with fins.

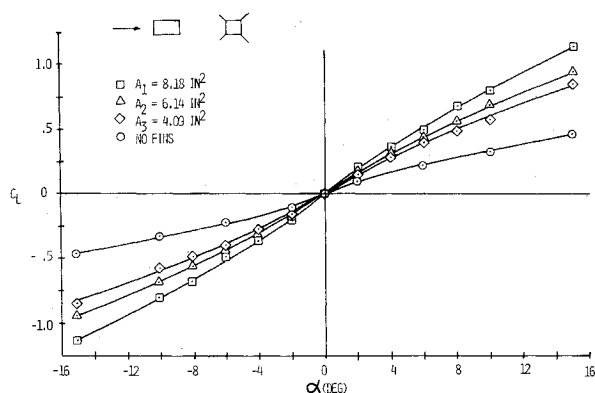


Fig. 1c Lift coefficient vs angle of attack for rectangular box.

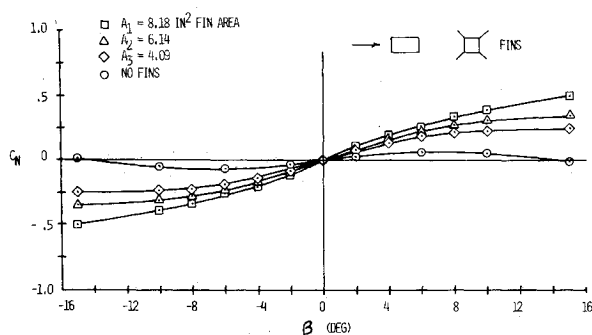


Fig. 1d Yaw moment coefficient vs side-slip angle for rectangular box.

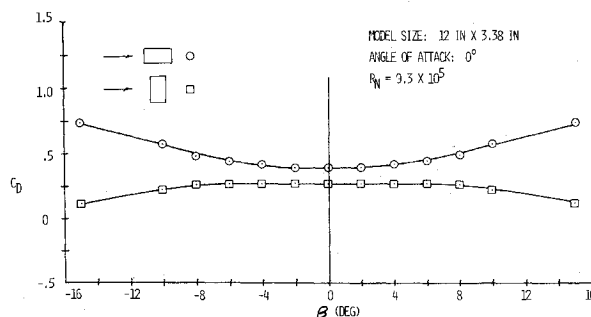


Fig. 2a Drag coefficient vs side-slip angle for cylinder.

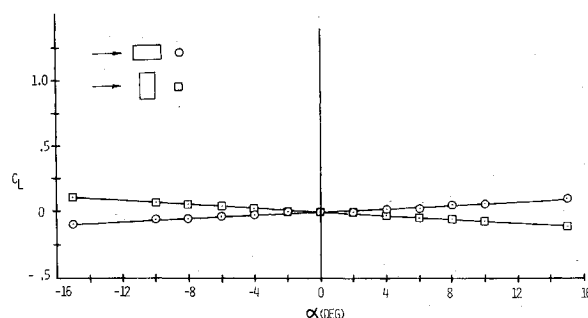


Fig. 2b Lift coefficient vs angle of attack for cylinder.

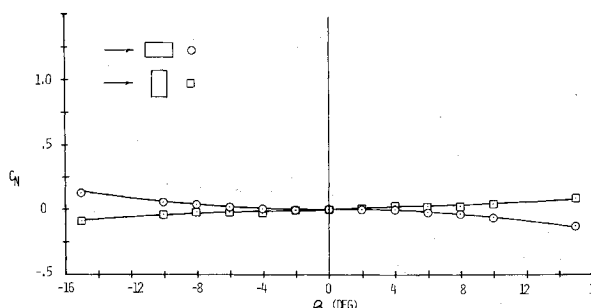
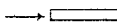
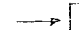


Fig. 2c Yaw moment coefficient vs side-slip angle for cylinder.

Table 1 Stability derivatives

Configuration	$C_{D_0}$	$C_{L_0}$	$C_{D_\alpha}$ (/deg)	$C_{L_\alpha}$ (/deg)	$C_{m_\alpha}$ (/deg)	$C_{y_\beta}$ (/deg)	$C_{l_\beta}$ (/deg)	$C_{n_\beta}$ (/deg)
Box - No Fins								
$r/w = 0$	.915	0	0	.0317	-.0117	-.0477	0	.0117
$r/w = .05$	.755	0	0	.0317	-.0117	-.0449	0	.0117
$r/w = .1$	.590	0	0	.0317	-.0117	-.0420	0	.0117
$r/w = .2$	.416	0	0	.0317	-.0117	-.0389	0	.0117
Box - Fins (square edged)								
$A_1 = 42.7 \text{ ft}^2$	.930	0	0	.0770	-.0400	-.0932	0	.0400
$A_2 = 32.1 \text{ ft}^2$	.930	0	0	.0633	-.0350	-.0795	0	.0350
$A_3 = 21.5 \text{ ft}^2$	.930	0	0	.0563	-.0325	-.0725	0	.0325
Cylinder								
	.890	0	0	.0063	.0006	-.0218	0	-.0006
	.760	0	0	-.0070	-.0040	-.0063	0	.0040

with the results of Szustak and Jenney<sup>14</sup> confirms again that the size effect on this type of body is not of major significance. This is due, of course, to the fact that the flow separates at the sharp corners and thus is not dependent on Reynolds Number.

Unlike the box, the force and moment characteristics for a cylinder, both in longitudinal and in cross flow, are heavily dependent on Reynolds Number. Lehmann<sup>16</sup> shows this effect in his results for three different values of Reynolds Number. The cylinder results shown in Fig. 2 are for a single Reynolds Number of  $9.3 \times 10^5$  which corresponds to the high range reported by Lehmann.

Tuft studies confirmed that the flow did indeed separate at the corners and that fins arranged in a crucifix form would be most effective for all model orientations. These studies further showed that rounding of all the edges smoothed the flow and, as expected, shifted the reattachment line forward, hence reducing the drag as shown in Fig. 1a. Rounding the edges had no measurable effect on any of the other aerodynamic coefficients.

Stability derivatives were obtained graphically from the force and moment coefficient curves and are shown in Table 1. It is not expected that Reynolds Number effects would significantly alter the values of the stability derivatives even for the right-circular cylinder.

### Equations of Motion

Appendix A shows that the linearized equations of motion for a rigid body being towed beneath a rotary winged aircraft flying at a constant velocity  $U_0$  (Fig. 3) are

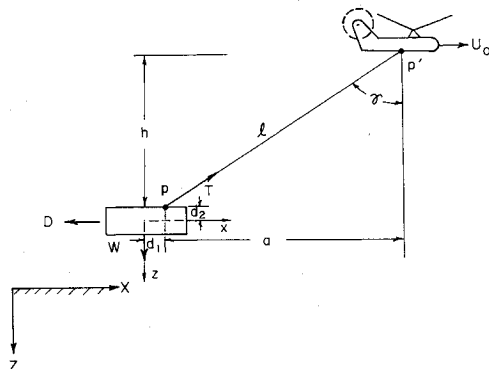


Fig. 3 Steady-state towing.

Longitudinal:

$$\begin{bmatrix} m\lambda - X_u & -X_w & -a/l & -Z_o & -X_o/a & 0 \\ -Z_u & m\lambda - Z_w & h/l & -mu_o\lambda + X_o & 0 & -X_o/a \\ +M_u & M_w & 0 & -B\lambda^2 & 0 & 0 \\ -1 & 0 & 0 & 0 & \lambda & 0 \\ 0 & -1 & 0 & U_o & 0 & \lambda \\ 0 & 0 & 0 & 0 & -a & h \end{bmatrix} \begin{bmatrix} u \\ w \\ \Delta T \\ \theta \\ x' \\ z' \end{bmatrix} = 0 \quad (1)$$

Lateral:

$$\begin{bmatrix} m\lambda - Y_v & U_o m\lambda - X_o & Z_o & -X_o/a \\ -L_v & 0 & A\lambda^2 & 0 \\ -N_v & C\lambda^2 & 0 & 0 \\ -1 & -U_o & 0 & \lambda \end{bmatrix} \begin{bmatrix} v \\ \psi \\ \phi \\ y' \end{bmatrix} = 0 \quad (2)$$

$$\lambda = d/dt$$

Where  $m$  is the mass of the towed body;  $l$  the length of the cable;  $a$  and  $h$  the horizontal and vertical distances between the two attachment points  $P$  and  $P'$ ;  $A, B$ , and  $C$  the moments of inertia of the towed body about the  $x, y$ , and  $z$  axes, respectively;  $u, v$ , and  $w$  the linear perturbation velocities along  $x, y$ , and  $z$ , respectively;  $\theta, \psi$ , and  $\phi$  the angles of pitch, yaw, and roll;  $x', y'$ , and  $z'$  the linear displacements of the center of mass of the towed body from the steady-state flight;  $X, Y, Z, L, M$ , and  $N$  the aerodynamic forces and moments along  $x, y$ , and  $z$ , respectively;  $X_u, Y_v$ , etc. the changes in the aerodynamic forces and moments due to changes in the linear velocities;  $\Delta T$  the change in the cable tension from its steady-state value.

In deriving these equations several assumptions were made. First, the towing craft was assumed to be flying straight and level. Second, the aerodynamic forces and moments are such that the lateral and longitudinal degrees of freedom can be uncoupled. Third, the towed body is outside the wake of the helicopter rotor. Last, the rigid body motion of the towed body is uncoupled from the dynamical motion of the cable. The assumption of symmetric flight was borne out by the experimental data obtained in this study.

For the kinds of systems under consideration here, the towed weight is assumed to be much greater than the cable weight. Under these conditions it is not difficult to show that the natural frequencies of the cable are much

less than the natural frequencies of the rigid-body motion; thus, the motions can be assumed to be uncoupled. This result was verified rigorously in Ref. 11. Appendix B discusses an approximate method for accounting for cable dynamics.

### Stability Analysis

The characteristic equations for the lateral and longitudinal motion of the towed body are obtained by expanding the determinant of the coefficients in Eqs. 1 and 2. For the case of steady-state flight, an examination of the wind-tunnel test results and the steady-state equations of motion shows that for the equilibrium condition of  $\alpha = \beta = 0$ ,  $Z_o = Z_u = M_u = L_v = 0$ . Thus, for the longitudinal mode,

$$mB\ell^2\lambda^4 - (a^2BZ_w + h^2BX_u)\lambda^3 - [\ell^2mU_oM_w + (\ell^2/a)BX_o]\lambda^2 + (h^2U_oX_uM_w + a^2M_wX_o)\lambda + [(\ell^2/a)U_oX_oM_w] = 0 \quad (3)$$

for the lateral mode,

$$Cm\lambda^4 - CY_v\lambda^3 + (N_v mU_o - X_o C/a)\lambda^2 - N_v X_o\lambda - X_o U_o N_v/a = 0 \quad (4)$$

Both of these equations are in the form

$$a_o\lambda^4 + a_1\lambda^3 + a_2\lambda^2 + a_3\lambda + a_4 = 0 \quad (5)$$

A necessary and sufficient condition for stability in this case is that all the coefficients of  $\lambda$  be positive and that

$$a_3(a_1a_2 - a_oa_3) - a_1^2a_4 > 0 \quad (6)$$

For the box and cylinder under discussion here, the coefficients  $a_o, a_1, \dots, a_4$  are all positive; hence, all that is required for stability is that Eq. (6) be satisfied. For the longitudinal degrees of freedom this condition takes the form

$$C_{L_\alpha} C_m C_D [amc C_m (2h^2 + a^2) + a^2B(C_D + C_{L_\alpha}) + 2Bh^2C_D] > 0 \quad (7)$$

while for the lateral degrees of freedom it takes the form

$$mbC_n + (C/a)C_y > 0 \quad (8)$$

The nondimensional stability derivatives,  $C_{L_\alpha}$ ,  $C_{m_\alpha}$ , etc., are defined in the Nomenclature.

### Results

For the 8 ft  $\times$  8 ft  $\times$  20 ft cargo container without fins, the longitudinal stability requirement, Eq. (7), reduces to the following

$$\ell > \frac{(C_D - 57.3 C_{L_\alpha})(1.933 s^2 \gamma) - 3.866 C_D}{57.3(2 - \sin^2 \gamma) C_{m_\alpha} \sin \gamma} \quad (9)$$

where

$$\gamma = \tan^{-1}(D/W) \quad (10)$$

$D/W$  is, of course, the drag-to-weight ratio of the towed body during steady-state conditions, and  $\gamma$  is the steady-state towing angle (Fig. 3).

The lateral stability condition, Eq. (8), becomes

$$\ell > \frac{-1.933 C_y}{C_n \sin \gamma} \quad (11)$$

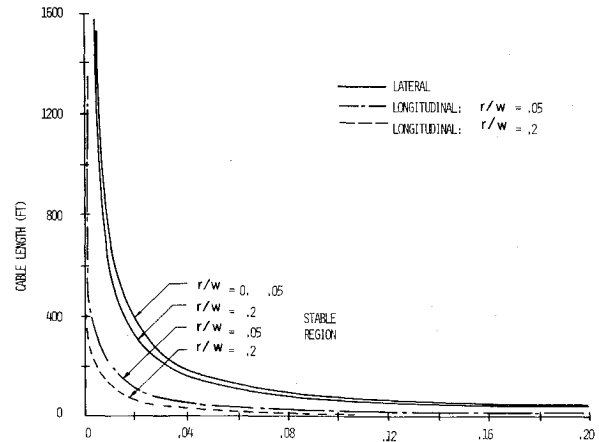


Fig. 4 Lateral and longitudinal stability of box—no fins.

The stability derivatives,  $C_{L_\alpha}$ ,  $C_{m_\alpha}$ ,  $C_{y_\beta}$ , and  $C_{n_\beta}$ , are in units of (degree) $^{-1}$ .

These results are plotted in Figs. 4–6. It is seen from these plots that the most important stability parameters are the drag-to-weight ratio of the towed body and the length of the cable. These curves show that as the drag-to-weight ratio increases, the cable length required for stability decreases. Thus, for a given cable length and towed weight, a minimum speed exists below which motion is unstable.

Figure 4 shows both the lateral and longitudinal stability plots for the case of the container without stabilizing fins. It is seen here that the lateral mode is the more critical one, that is, a cable length and drag-to-weight ratio that ensures lateral stability also ensures longitudinal stability.

Figures 5 and 6 show the effect of the stabilizing fins. Above a drag-to-weight ratio of 0.02 it is seen that the fins allow a reduction in cable length of some 30–50%. It is also seen that there is no great advantage in going to larger fins.

As a practical example consider the case of the S-64E helicopter which has a cruise speed of 160 fps and a 100-ft cable. For a 20,000 lb cargo container with a drag coefficient of 0.825 the drag-to-weight ratio is 0.08. In this case, Fig. 4 shows that no fins are required for stability. For a 30,000 lb container, stabilizing fins would be required.

An analysis similar to the one described above was also carried out for a right-circular cylinder of length 20 ft and a diameter of 5.4 ft. In all cases, the container was found to be unstable. While previous work<sup>16</sup> indicates that it may have been possible to find a Reynolds number for

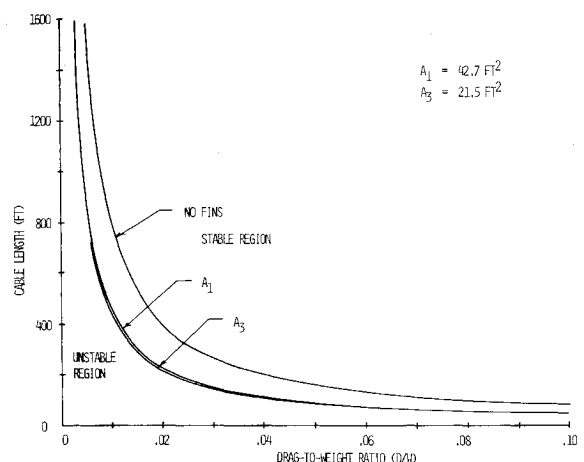


Fig. 5 Lateral stability of box with fins.

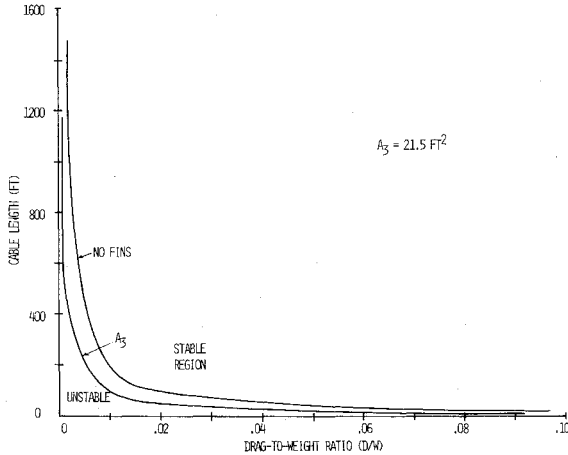


Fig. 6 Longitudinal stability of box with fins.

which a statically stable cylinder exists, this possibility was not pursued.

It is interesting to compare the single-point suspension system results obtained here with the qualitative results obtained by Szustak and Jenney<sup>14</sup> for two- and four-point suspension systems. For the single-point system the present results show that long cables, high speeds, and light loads are required for stability. For the two- and four-point systems Szustak and Jenney conclude that short cables, low speeds, and heavy loads are required. The present results agree, however, with the single-point suspension results obtained experimentally by Etkin<sup>5</sup> for lateral stability of a streamlined body. Etkin's work shows that two stable regions exist, a low- and a high-speed region, separated by an intermediate unstable region. The low-speed region was not obtained in the present work due to the neglect of the change in yaw moment with yaw velocity,  $N_r$ .

In summary, then, it is seen that if towing is to be considered as an effective mode of transportation additional operational methods must be devised and investigated. Such investigations are currently being conducted by the authors.

#### Appendix A: Equations of Motion of the Towed Body

Before deriving the equations of motion of the towed body, it is necessary to define two coordinate systems. First, an  $X', Y', Z'$  coordinate system fixed to the surface of the Earth in such a manner that  $Z'$  points downward,  $X'$  points to the right, and  $Y'$  such that a right-handed coordinate system is formed. An  $x, y, z$  right-handed coordinate system whose origin is fixed to the c.m. of the towed body. The  $x$  axis points along the longitudinal axis of symmetry of the body,  $z$  points towards the surface of the Earth, and  $y$  is such that a right-handed system is completed (Fig. 3).

If the orientation of the towed body with respect to the Earth fixed system is obtained via the standard aircraft Euler angles,<sup>17</sup> then unit vectors in the two coordinate systems are related as follows:

$$\begin{bmatrix} \bar{i} \\ \bar{j} \\ \bar{k} \end{bmatrix} = \begin{bmatrix} c\theta c\psi & c\theta s\psi & (-s\theta) \\ (s\phi s\theta c\psi - c\phi s\psi) & (s\phi s\theta s\psi + c\phi c\psi) & (s\phi c\theta) \\ (c\phi s\theta c\psi + s\phi s\psi) & (c\phi s\theta s\psi - s\phi c\psi) & (c\phi c\theta) \end{bmatrix} \begin{bmatrix} \bar{I} \\ \bar{J} \\ \bar{K} \end{bmatrix} \quad (A1)$$

where  $\bar{I}, \bar{J}, \bar{K}$  and  $\bar{i}, \bar{j}, \bar{k}$  are unit vectors along the  $X, Y, Z$  and the  $x, y, z$  axes, respectively, and for brevity the convention  $c\theta = \cos\theta$ ,  $s\theta = \sin\theta$ , etc., is used.

If the  $xz$  plane is a plane of symmetry, then the equations of motion for the towed body are given by

$$\begin{aligned} X - mgs\theta + T_x &= m(\dot{U} + QW - RV) \\ Y + mgc\theta s\phi + T_y &= m(\dot{V} + RU - PW) \\ Z + mgc\theta c\phi + T_z &= m(\dot{W} + PV - QU) \\ L + M_T^x &= A\dot{P} - E\dot{R} + QR(C - B) - EPQ \\ M + M_T^y &= B\dot{Q} + RP(A - C) + E(P^2 - R^2) \\ N + M_T^z &= C\dot{R} - E\dot{P} + PQ(B - A) + EQR \\ \dot{P} &= \dot{\phi} - \dot{\psi}s\theta \\ \dot{Q} &= \dot{\theta}c\phi + \dot{\psi}c\theta s\phi \\ \dot{R} &= \dot{\psi}c\theta c\phi - \dot{\theta}s\phi \end{aligned} \quad (A2)$$

where the  $x, y$ , and  $z$  components, respectively, of the linear and angular velocity of the body are denoted by  $U, V, W$  and  $P, Q, R$ ; the aerodynamic forces and moments by  $X, Y, Z$  and  $L, M, N$ ; and the moments of inertia by  $A, B$ , and  $C$ . The product of inertia is denoted by  $E$ .

The forces and moments due to the cable are denoted by  $T_x, T_y, T_z, M_T^x, M_T^y$ , and  $M_T^z$ , and are given by the following expressions:

$$\begin{aligned} T_x &= T/\ell(ac\theta c\psi + hs\theta) \\ T_y &= T/\ell[(s\phi s\theta c\psi - c\phi s\psi)a - s\phi c\theta h] \\ T_z &= T/\ell[(c\phi s\theta c\psi + s\phi s\psi)a - c\phi c\theta h] \\ M_T^x &= T/\ell(d_1h - d_2a)c\theta s\psi \\ M_T^y &= T/\ell(d_1h - d_2a)(s\phi s\theta s\psi + c\phi c\psi) \\ M_T^z &= T/\ell(d_1h - d_2a)(c\phi s\theta s\psi - s\phi c\psi) \end{aligned} \quad (A3)$$

where  $T$  represents the tension in the cable and  $d_1$  and  $d_2$  locate the attachment point of the cable to the slung load, in the  $X, Y, Z$  axis system.

The velocity components of the towed body along the  $X, Y, Z$  axis system are given by

$$\begin{aligned} \dot{X}' &= U' = Uc\theta c\psi + V(s\phi s\theta c\psi - c\phi s\psi) + W(c\phi s\theta c\psi + s\phi s\psi) \\ \dot{Y}' &= V' = Uc\theta s\psi + V(s\phi s\theta s\psi + c\phi c\psi) + W(c\phi s\theta s\psi - s\phi c\psi) \\ \dot{Z}' &= W' = -Us\theta + Vs\phi c\theta + Wc\phi c\theta \end{aligned} \quad (A4)$$

If the steady-state flight conditions are given by

$$U = U_0$$

and

$$V = W = P = Q = R = \theta = \phi = \psi = 0$$

then the equations of motion during steady-state flight are

$$\begin{aligned} 0 &= X_0 + T_0(a/\ell) \\ 0 &= Y_0 \\ 0 &= Z_0 + mg - T_0(h/\ell) \\ 0 &= L_0 \\ 0 &= M_0 + (T_0/\ell)(d_1h - d_2a) \\ 0 &= N_0 \end{aligned} \quad (A5)$$

If the towed body becomes slightly disturbed from its steady-state equilibrium condition, such that

$$\begin{aligned} U &= U_0 + u & P &= p & \theta &= \theta \\ V &= v & Q &= q & \phi &= \phi \\ W &= w & R &= r & \psi &= \psi \end{aligned}$$

and

$$\begin{aligned} X &= X_0 + \Delta X & L &= L_0 + \Delta L & T &= T_0 + \Delta T \\ Y &= Y_0 + \Delta Y & M &= M_0 + \Delta M \\ Z &= Z_0 + \Delta Z & N &= N_0 + \Delta N \end{aligned}$$

then, upon substituting these expressions into Eqs. (A2) and (A4) and subtracting out the steady-state equations, the following results are obtained

$$\begin{aligned} m\ddot{u} &= \Delta X - mg\theta + \Delta T_x \\ m[\dot{v} + rU_0] &= \Delta Y + mg\phi + \Delta T_y \\ m[\dot{w} - qU_0] &= \Delta Z + \Delta T_z \\ A\dot{p} - E\dot{r} &= \Delta L + \Delta M_{T_x} \\ Bq &= \Delta M + \Delta M_{T_y} \\ C\dot{r} - E\dot{p} &= \Delta N + \Delta M_{T_z} \\ \dot{\theta} &= q \\ \dot{\phi} &= p \\ \dot{\psi} &= r \end{aligned} \quad (A6)$$

$$\begin{aligned} u' &= u \\ v' &= v + U_0\theta \\ w' &= w - U_0\theta \end{aligned}$$

where

$$\begin{aligned} \Delta X &= X_u u + X_w w \\ \Delta Y &= Y_v v \\ \Delta Z &= Z_u u + Z_w w \end{aligned}$$

$$\begin{aligned} \Delta L &= L_v v \\ \Delta M &= M_u u + M_w w \\ \Delta N &= N_v v + N_r r \end{aligned}$$

$$\begin{aligned} \Delta T_x &= -(T_0/\ell)[x' - (h + d_2)\theta] + (\Delta T/\ell)a \\ \Delta T_y &= -(T_0/\ell)[(a + d_1)\psi + Y' + (h + d_2)\phi] \\ \Delta T_z &= -(T_0/\ell)[z' - (a + d_1)\theta] - (\Delta T/\ell)h \end{aligned}$$

and

$$\begin{aligned} \Delta M_{T_x} &= d_2'\Delta T_y \\ \Delta M_{T_y} &= -d_1'\Delta T_z - d_2'\Delta T_x \\ \Delta M_{T_z} &= d_1'\Delta T_y \end{aligned}$$

The lower case letters,  $u, v, w$ , etc., denote, of course, small deviations from steady state.  $X_u, X_w$ , etc., denote changes in the aerodynamic forces and moments due to changes in velocity.

If the towing cable is considered to be inextensible, then the displacements of the towed body from its steady-state conditions are not independent but are instead related by the following equation

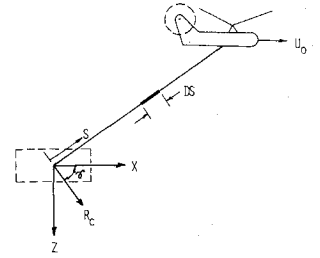
$$\begin{aligned} |\bar{\rho}_{12}|^2 &= a^2 + h^2 = [(a - x') + (h + d_2)\theta]^2 + \\ &+ [-Y' - \psi(a + d_1) - (h + d_2)\phi]^2 + [-(h + z') + (a + d_1)\theta]^2 \end{aligned}$$

Upon expanding the above and retaining only the first-order terms, the following equation of constraint is obtained

$$-ax' + hz' + \theta[a(h + d_2) - h(a + d_1)] = 0 \quad (A7)$$

The equations necessary for a small-perturbation stability analysis of the towed system have now been obtained and are given by Eqs. (1) and (2) for the case where  $d_1 = d_2 = 0$ .

Fig. 7 Cable inertia effects.



## Appendix B: Inertia Effects of the Cable

When the weight of the cable is much less than the weight of the towed body, the cable can be assumed to execute a rigid-body rotation about the aircraft attachment point, due to a perturbation in the acceleration of the attachment point of the towed body.

If  $a'$  represents the component of acceleration of the center of mass of the towed body in the longitudinal plane, then the acceleration,  $a_s$ , of a small element of the cable,  $ds$  at a distance  $s$  from the towed body attachment point (Fig. 7), is

$$a_s = [(\ell - s)/\ell]a' \quad (B1)$$

Thus, the total cable inertial force due to this perturbation is given by

$$F_c = m_c a' \int_0^\ell \frac{(\ell - s)}{\ell} ds = \frac{m_c a' \ell}{2} \quad (B2)$$

where  $m_c$  is the weight per unit length of the cable and  $F_c$  is perpendicular to the cable. Equation (B1) shows that the inertia force has a triangular distribution, with its maximum value at  $s = 0$ . Thus, at the end  $s = 0$ , the reaction force on the cable due to this inertia loading must be  $2/3 F_c$  or

$$R_c = (1/3)m_c a' \ell \quad (B3)$$

The components in the  $x$  and  $y$  direction are given by

$$R_{c_x} = R_c \cos \gamma = (1/3)m_c \ell \ddot{x} = (1/3)m_c \ell \ddot{u}$$

$$R_{c_z} = R_c \sin \gamma = (1/3)m_c \ell \ddot{z} = (1/3)m_c \ell (\ddot{w} - \theta U_0) \quad (B4)$$

Similarly, due to a perturbation in the  $y$  direction, the reaction at  $s = 0$  is

$$R_{c_y} = (1/3)m_c \ell \ddot{y} = (1/3)m_c \ell (\dot{v} + \dot{\psi} U_0) \quad (B5)$$

Due to these reaction forces, equal and opposite forces must act on the towed vehicle itself. The translational equations of motion in this case become

$$\begin{aligned} m\ddot{u} &= \Delta X - mg\theta + \Delta T_x - (1/3)m_c \ell \ddot{u} \\ m(\dot{v} + \dot{\psi} U_0) &= \Delta Y + mg\phi + \Delta T_y - (1/3)m_c \ell (\dot{v} + \dot{\psi} U_0) \\ m(\dot{w} - \theta U_0) &= \Delta Z + \Delta T_z + (1/3)m_c \ell (\dot{w} - \theta U_0) \end{aligned} \quad (B6)$$

These equations are identical to those obtained earlier except that the acceleration terms are now multiplied by  $(m + 1/3 m_c \ell)$ . Thus, Eqs. (7) and (8) remain the same except that  $m$  is replaced by  $(m + 1/3 m_c \ell)$ . The expressions for the critical cable length are now slightly altered by the appearance of the term  $s\gamma[1 + 1/3 (m_c \ell/m)]$  in place of  $s\gamma$  in the denominator of Eqs. (9) and (11).

Thus, it is seen that when the weight of the cable is much less than the weight of the towed body, the critical lengths calculated earlier are approximately correct and on the conservative side.

## References

- <sup>1</sup>Glauert, H., "The Stability of a Body Towed by a Light Wire," R&M 1312, Feb. 1930, Aeronautical Research Committee, Farnborough, England.
- <sup>2</sup>Glauert, H., "The Form of a Heavy Flexible Cable Used for Towing a Heavy Body below an Aeroplane," R & M 1592, Feb. 1934, Aeronautical Research Committee, Farnborough, England.
- <sup>3</sup>O'Hara, F., "Extension of Glider Tow Cable Theory to Elastic Cables Subject to Air Forces of a Generalized Form," R & M 2334, Nov. 1945, Aeronautical Research Council, Farnborough, England.
- <sup>4</sup>Phillips, W. H., "Theoretical Analysis of Oscillations of a Towed Cable," TN 1796, 1949, NACA.
- <sup>5</sup>Etkin, B. and Mackworth, J. C., "Aerodynamic Instability of Non-Lifting Bodies Towed Beneath an Aircraft," TN 65, 1963, Institute of Aerophysics, University of Toronto, Toronto, Ontario, Canada.
- <sup>6</sup>Shanks, R. E., "Investigation of the Dynamic Stability and Controllability of a Towed Model of a Modified Half-Cone Reentry Vehicle," TN D-2517, 1965, NASA.
- <sup>7</sup>Shanks, R. E., "Experimental Investigation of the Dynamic Stability of a Towed Parawing Glider," TN D 1614, 1963, NASA.
- <sup>8</sup>Shanks, R. E., "Experimental Investigation of the Dynamic Stability of a Towed Parawing Glider Air Cargo Delivery System," TN D-2292, 1964, NASA.
- <sup>9</sup>Sohne, W., "Directional Stability of Towed Airplanes," TM 1401, 1956, NACA.
- <sup>10</sup>Reid, W. P., "Stability of a Towed Object," *SIAM Journal of Applied Mathematics*, Vol. 15, No. 1, Jan. 1967, pp. 1-2.
- <sup>11</sup>Huffman, R. R. and Genin, J., "The Dynamical Behaviour of a Flexible Cable in a Uniform Flow Field," *Aeronautical Quarterly*, Vol. XXII, Pt. 2, May 1971, pp. 183-195.
- <sup>12</sup>Casarella, M. J. and Parsons, M., "Cable Systems Under Hydrodynamic Loading," *MTS Journal*, Vol. 4, No. 4, 1970, pp. 27-44.
- <sup>13</sup>Sheldon, D. F., "A Study of the Stability of a Plate-Like Load Towed Beneath a Helicopter," *Journal of Mechanical Engineering Science*, Vol. 13, No. 5, 1971, pp. 330-343.
- <sup>14</sup>Szustak, L. S. and Jenny, D. S., "Control of Large Crane Helicopters," *Journal of the American Helicopter Society*, Vol. 16, No. 3, July 1971, pp. 11-22.
- <sup>15</sup>Hutto, A. J., "Qualitative Report on Flight Test of a Two-Point External Load Suspension System," Reprint 473, Presented at the 26th Annual National Forum of the American Helicopter Society, Washington, D.C.
- <sup>16</sup>Lehmann, J. W., "The Aerodynamics Characteristics of Non-Aerodynamic Shapes," M.S. thesis, GAM/AE/68-6, June 1968, School of Engineering, Air Force Institute of Technology, Wright-Patterson Air Force Base, Ohio.
- <sup>17</sup>Etkin, B., *Dynamics of Flight*, Wiley, New York, 1958, Chap. 4.

FEBRUARY 1973

J. AIRCRAFT

VOL. 10, NO. 2

## Far-Field Structure of Aircraft Wake Turbulence

W. H. Mason\* and J. F. Marchman III†

Virginia Polytechnic Institute and State University, Blacksburg, Va.

Detailed mean flow measurements were obtained at stations up to thirty chordlengths downstream in an airfoil trailing vortex using a yawhead pressure probe in the Virginia Tech Six-Foot Subsonic Tunnel. Mass injection at the wingtip was shown to hasten the vortex decay. A theoretical method has been developed to show the effect of wing circulation distribution on the structure of the outer portion of the vortex and excellent agreement with the experimental data is demonstrated.

## Nomenclature

$a$	= probe radius
$A_C$	= core radius
$A_n$	= coefficients of Fourier series of wing circulation
$AR$	= aspect ratio
$C$	= wing chord
$F$	= force between probe and vortex
$J_o$	= moment of inertia of flat sheet about plane of symmetry
$J_{y_1}$	= momental inertia of flat sheet about c.g.
$J_{r_1}$	= moment of inertia after rollup
$K$	= ratio of effective to kinematic viscosity
$\dot{m}$	= mass flow
$P_{st}$	= static pressure
$P_o$	= stagnation pressure
$\Delta P$	= pressure difference across yawhead probe tip
$Q$	= dynamic pressure
$r, \theta, z$	= cylindrical coordinate directions
$Re$	= Reynolds number
$t$	= time
$s$	= wing semispan
$V_x, V_y, V_z$	= Cartesian velocities
$V_r, V_\theta, V_z$	= cylindrical velocities

$V_\infty$	= freestream undisturbed velocity
$x, y, z$	= cartesian coordinate directions
$\bar{y}$	= c.g. of flat vorticity sheet
$\gamma$	= flat vorticity sheet strength
$\epsilon_T$	= wing-tip twist angle
$\lambda$	= wing taper ratio
$\nu_T$	= kinematic viscosity
$\nu^T$	= effective (turbulent) kinematic viscosity
$\rho$	= mass density

## Introduction

THE prediction of the turbulence trail of an aircraft has become extremely important with the introduction of "Jumbo Jet" class aircraft into terminal areas because of the potential hazard to other aircraft encountering them in flight. The FAA has initiated longer time spacing between large jet aircraft and following aircraft to assure safe separation and reduce the possibility of vortex encounter. This longer time spacing reduces the number of operations possible at busy airports and compounds the already serious traffic problem. In addition, even though the next generation of avionics is expected to allow aircraft to land and take off with significantly less spacing, wake turbulence could become the major limiting factor prohibiting the achievement of the maximum airport capacity afforded by improved equipment. Therefore, in order to minimize the wait time of aircraft on the ground and in the air, with its accompanying noise and chemical

Presented as Paper 72-40 at the AIAA 10th Aerospace Sciences Meeting, San Diego, Calif., January 17-19, 1972; submitted February 14, 1972; revision received December 14, 1972. This research was supported by NASA Grant NGL 47-004-067.

Index category: Aircraft Aerodynamics.

\*Graduate Student.

†Associate Professor, Associate Member AIAA.